A MECHANIZED PEDIATRIC ELBOW JOINT POWERED BY A DE-BASED ARTIFICIAL SKELETAL MUSCLE *

A. Behboodi, *Member IEEE*, C. DeSantis, J. Lubsen, S.C.K. Lee,

***Abstract*— To increase the acceptability of exoskeletons, there is growing attention toward finding an alternative soft actuator that can safely perform at close vicinity of the human body. In this study, we investigated the capability of the dielectric elastomer actuators (DEAs), for muscle-like actuation of rehabilitation robots. First, an artificial skeletal muscle was configured using commercially available stacked DEAs arranged in a 3x4 array of three parallel fibers consisting of four DEAs connected in series. The shortening and force generation capabilities of this artificial muscle were then measured. An alternate 3x5 version of this muscle was mounted on the forearm of an upper extremity phantom model to actuate its elbow joint. The actuation capability of this muscle was then tested under various tensile loads, 1 N to 4 N, placed at the center of mass of the forearm+hand of the phantom model. The active range of motion and angular velocity of the phantom model's tip of the hand were measured using a motion capture system. The 3×4 artificial muscle produced 30.47 N of force and 5.3 mm of maximum shortening. The 3x5 artificial muscle was capable of actuating the elbow flexion 19.5º with 16.2 º/s angular velocity in the sagittal plane, under a 1 N tensile load. The active range of motion was substantially reduced as the tensile loads increased, which limits the capability of these muscles in the current upper extremity exoskeleton design.**

I. INTRODUCTION

Modern concepts of rehabilitation support the use of intensive, repetitive, and task-oriented approaches aimed at restoring upper extremity disability [1]. Intense repetitions of coordinated motor activities, however, constitute a significant time burden for therapists assisting patients, which may not be reimbursed by third-party payers. Mass practice, therefore, is difficult to achieve during a typical therapy session. To facilitate practice, research studies present a wide variety of rehabilitation devices [2]. Assistive robots with the ability to perform repetitive tasks with patients are among these technically advanced devices. The more automated an assistive robot, the less supervision is needed. While able to increase the independence of the user in the performance of activities of daily living (ADLs), an assistive robot may have the added benefit to increase the dosage of interaction with the environment and others that consequently may result in more cognitive, social, and motor development. Additionally, because kinematic and kinetic data can be derived from the closed-loop systems used to control such robots, the data can contribute to the understanding of how different treatment variables (dosage, amount, type of assistance provided) may influence motor learning and recovery for their users. Robots can also be used in combination with computer gaming environments to motivate training and provide quantitative feedback [3]. Thus, the use of robots is getting more and more attention in rehabilitation engineering.

Exoskeleton devices for the arms, including the ARMin [4], MIME [5], T-WREX [6], and MIT-Manus [7] have shown promising rehabilitation outcomes and resulted in the development of commercial products such as Armeo Power, and Armeo Spring (Hacoma AG, Switzerland), the commercial verions of ARMin and T-WREX, respectively (Fig. 1, (a) and (b)). These devices, however, are not practical for at-home use, and their size and cost limit their practicality for widespread use [8]. Because healthcare delivery is shifting away from clinical facilities and into the community, there is a growing need for technologies for at-home interventions and devices, such as assistive exoskeletons, to assist ADLs [9].

The T-WREX [6], originally designed for such purposes, and its pediatric version P-WREX, are smaller and simpler to use compared to their powered counterparts. They, however, cannot generate motion and are thereby limited in their capabilities [10]. Alternatively, the MyoPro (Myomo, Cambridge, MA, USA), an EMG-triggered elbow brace [11], is one of the only commercially available powered exoskeletons, which showed efficacy for at-home rehabilitation in controlled pilot studies [9] (Fig.1, (c)).

Most assistive exoskeletons developed as rehabilitation robots lack natural feel; that is, they are heavy, bulky, noisy, and rigid structures [9]. Such designs are at high risk for dissatisfaction, unacceptance, and finally, abandonment of the device, especially in pediatric populations. The development of next-generation rehabilitation robots must, therefore, use innovative technologies to address such concerns to lead to significant benefits [12]. The conventional actuators used in most exoskeletons consist of DC motors typically used in industrial applications that do not interact with the human body, and therefore, have structural drawbacks as previously mentioned. An effective orthosis must, in general, be silent,

* Research supported by Shriners Hospitals for Children Grant #87500-PHI-17 and #71011-18-PHL, National Institute of Health DE-CTR ACCEL Grant #U54-GM104941, and Foundation for the National Institute of Health Grant #P30 GM103333.

A. Behboodi is with the Venture Development Center and the Department of Physical Therapy at the University of Delaware, Newark, DE 19716 USA (phone: 302-831-7611; e-mail: ahadbeh@udel.edu).

C. DeSantis and J. Lubsen are with the Mechanical Engineering Department, University of Delaware, Newark, DE 19716 USA (e-mails: codyd@udel.edu and jlubsen@udel.edu).

S. C. K. Lee is with Departments of Physical Therapy, Biomedical Engineering, and Interdisciplinary Graduate Program in Biomechanics and Movement Science, University of Delaware, Newark, DE 19716 USA, and Shriner's Hospital for Children, Philadelphia, PA 19140 (e-mail: slee@udel.edu).

Figure 1. Example of commercially available exoskeletons (a) Aremo Spring.(b) Armeo Power.(c) Myomo. The Armoe devices, although versatile, are bulky, expensive and complex.

those lightweight, compliant, and portable [13]. Because existing exoskeletons are structurally rigid, they present challenges for safe interactions with humans. In contrast, a revised approach using softer materials has the potential to exhibit greater adaptation, sensitivity, and agility of rehabilitation robots. Through the use of soft sensors, actuators, and structures, the user's natural degrees of freedom for movement would be less constrained [14].

Among all present soft actuator designs, one of the most suitable candidate designs for artificial muscles appears to be electroactive polymer actuators (EPA) [15]. EAPs include dielectric elastomer actuators (DEAs) [16] that enable the design of mechanical systems with a soft feel and an external envelope (size and shape) approximating that of a natural limb [17]. The requirement for a "natural" look and feel is important to the goal of making the artificial or assisted limb feel integrated with the body. DEAs consist of a compliant capacitor, of which an elastic dielectric is sandwiched between two mechanically compliant electrodes (Fig. 2). When a DC voltage is applied to the electrodes, the resultant Maxwell pressure, i.e., the pressure between two oppositely charged plates due to electrostatic force, squeeze the dielectric in the thickness dimension.

DEAs have unique properties, including large electrically-induced area strains (120-380%), large electrically-induced stresses (up to about 3 MPa), and low response times (1ms or lower with low-loss elastomers) [18], which exceed the characteristics of natural muscle. Fundamentally, both DEAs and natural muscle consist of soft viscoelastic matter that can generate forces in response to electrical stimuli [19]. The force and strain of DEAs can be electrically modulated to control their stiffness [20]. Inherently compliant DEAs can mimic the agonist/antagonist muscle pairs found in nature so that concentric contraction of one artificial skeletal muscle is taken up by eccentric contraction in the other [21]. This property is applicable in modulating joint stiffness over ranges wider than

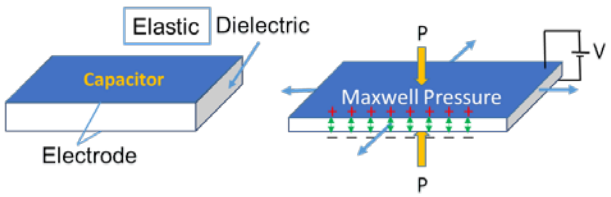

Figure 2. Maxwell pressure and the resultant compression

possible with a single actuator [17]. Finally, human motor control uses sensory, i.e., proprioceptive, feedback from muscle spindles and Golgi tendon organs within the muscles. By combining proprioception with actuation, natural muscle is multi-functional [22]. Similarly, in DEAs, elastomer deformations are inextricably linked to changes in electrical parameters that include capacitance and resistance, so the state of strain can be inferred by sensing these changes and enable closed-loop control without any additional sensors. In contrast, common actuators in robotics need independent sensing devices for closed-loop control, which increases the size and complexity of the system with a higher number of components. The DEA's unique properties are particularly suitable for developing light, soft, and inconspicuous mechanical systems with noise-free actuation and are of immediate interest for use in active orthoses and prostheses designs. Carpi et al. previously showed the possibility of using dielectric elastomers in orthoses design [23]–[25].

From the perspective of artificial skeletal muscle designs, one of the most suitable DEA configurations for exoskeletons is the stacked actuator. The hierarchic structure of human skeletal muscles is considered a useful analogous actuator model of numerous sarcomeres in series [26]. Similarly, stacked DEAs (SDEAs) are capable of effectively coupling the deformations of individual DE layers to provide linear actuation, and as with sarcomeres, employing a large number of DEA layers amplifies linear displacement. The novel and highly reliable SDEA invented by Dr. Kovacs et al. [27], of CTsystems, represents the most appropriate DEA design when noiseless and linear contractions of a soft actuator are required in close proximity to humans. CTsystems is the first and only mass production manufacturer of commercial DEAs having a stacked muscle-like configuration. Behboodi et al. benchmarked this group of actuators and compared them to the biological skeletal muscle [28]. This study was the first that assessed the capability of CTsystems' SDEAs (CT-SDEAs) to act as an artificial biceps muscle. These novel and reliable actuators have only recently become available, thus opening the way for the development of novel rehabilitation robotic devices that take advantage of the touted characteristics DEAs, which have the potential to revolutionize the field of rehabilitation robotics. The specifications of these actuators can be found in Table I.

The ultimate aim of this work is to develop an active pediatric upper extremity exoskeleton made of soft materials,

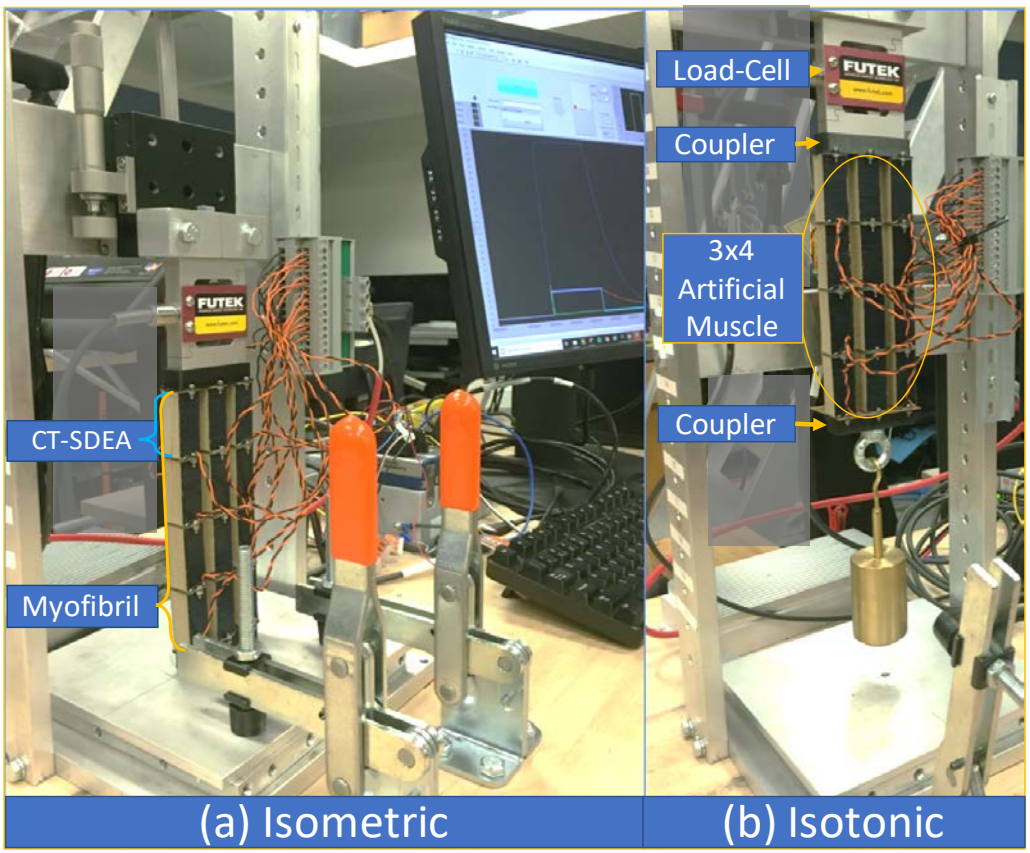

Figure 3. 3x4 artificial muscle was tested under isometric and isotonic testing setup. (a) the muscle was fix to the FUTEK Load cell and the test rig frame for the isometric testing. (b) the tensile loads were hung from the muscle, which was connected the load cell.

having a silent operation that enables ADL function and can provide directed mass practice activities for improving motor function. The present work consists of proof of concept experiments to mechanize a pediatric elbow joint using an artificial skeletal muscle composed of CT-SDEAs.

II. Methods

A. Configuring Artificial Skeletal Muscle

A 3x4 bundle of CT-SDEAs (three parallel fibers of four CT-SDEAs connected in series) was configured to form an artificial skeletal muscle. Similar to skeletal muscle, the artificial skeletal muscle configuration can be thought of having artificial sarcomeres (each DE layer in the CT-SDEA), motor units (each CT-SDEA), myofibrils (the CT-SDEAs connected in series), muscle fibers (the bundle of parallel artificial myofibrils), and proprioception, i.e., length self-sensing capability, in a single mechanical structure. This unique structural and functional similarity to skeletal muscle gives this artificial muscle the flexibility to 1) configure different numbers of artificial muscle sarcomeres (i.e., the number of layers within the CT-SDEA), artificial motor units (CT-SDEAs) and myofibrils (CT-SDEAs in series) to modulate force and displacement capability of the resultant muscle; 2) control the amount of force generation of the muscle by modulating the driving voltage and the number of activated motor units in the myofibrils; 3) create complex actuation by activating specific motor units in the artificial muscle myofibrils, and thereby, creating multiple degrees of freedom using one artificial muscle, e.g., by activating all the CT-DEAs the muscle contracts longitudinally, while by contracting any of the sides artificial myofibrils the muscle bends; and 4) controlling length modulation of the artificial muscle using "proprioceptive" length feedback.

B. Testing Procedure

The force and shortening of the previously mentioned artificial muscle configured in a 3x4 CT-SDEA array were measured using the method of Behboodi et al. [28] Then this artificial muscle was used to actuate an elbow joint of an upper extremity phantom model.

1) Measuring the force generation and shortening of the 3x4 artificial skeletal muscle.

A square activation waveform, with 1230 V amplitude, 5 s period, and 50% duty cycle, was used to activate the artificial muscle while measuring its contraction capabilities, i.e., force generation, shortening, and degree of elbow flexion.

Using the previously described testing setup (Fig. 3 and [28]), the force of the artificial muscle, generated by the square activation waveform, was recorded under isometric contraction conditions. During this condition, the length of the artificial muscle was held constant at its rest length, i.e., 156 mm, under no compression or extension, throughout the trials. This was produced by attaching one end of the artificial muscle with screws to a rigid frame and the other end to a load-cell (LSB302, 25 lb, FUTEK Advanced Sensor Technology, Inc., Imine, CA, USA) in a vertical position (Fig 3 (a)).

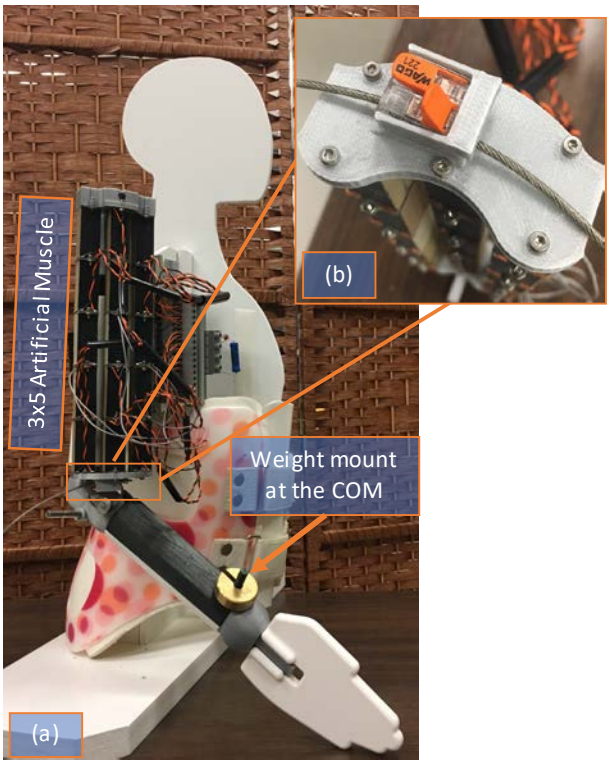

Figure 4. (a) The 3×5 muscle directly attached to the forearm of the phantom model. Different loads were mounted on the COM of the forearm+hand, 16 cm from the center of rotation. (b) The 3D printed end-plate with Wago connector casing, to attach three artificial myofibrils in parallel

Then muscle shortening was measured under various isotonic loaded conditions. For these conditions, the artificial muscle was secured to the load-cell in a vertical position, and a set of tensile loads were attached and hung from the artificial muscle using 3D printed couplers (Fig 3 (b)). The shortening distance for each loaded condition was measured using a laser displacement sensor (ILD 1420-25 Micro-Epsilon, Ortenburg, Germany) during the application of the activation waveform. The tensile loads used were 0.4 N (no-load condition), 3.3 N, and 6.8 N (g=10 m/s^2).

2) Implementing an Upper Extremity Phantom Model as the Exoskeleton Testing Platform.

For our pediatric exoskeleton development, we developed a phantom arm model to simulate the motion, size and weight of a hypothetical 95Th percentile 2-year-old boy by using Winter's anthropometric data [29] and World Health Organization (WHO) child growth standards [30] (Fig. 4). This model had a weight mount at the calculated center of mass (COM) of the forearm. The COM location from the forearm's center of rotation, 16.3 cm, was calculated based on hypothetical 95th percentile 2-year-old boy's standard height of 94 cm [30], and Winter's anthropometric data [29]. From these reference guidelines, we could simulate the weight of a 2-year-old forearm+hand, and during different loading conditions. The weight of the forearm + hand was calculated to be 338 g, i.e., 3.38 N. Thus, the 3.3 N and 6.8 N load was picked to emulate unloaded and loaded limb conditions, respectively.

3) Actuating the elbow joint of the phantom model by artificial skeletal muscle to measure the maximum achievable active range of elbow flexion.

To investigate the capability of the CT-SDEA-based artificial muscle in flexing the elbow, the muscle was mounted on the upper arm of the phantom model. Using a coated 1.6 diameter wire cable, the muscle was connected to the model's forearm, at 1 cm from the center of rotation, the elbow joint. A Wago connector (WAGO Kontakttechnik GmbH & Co. KG, Minden, Germany) were used to secure and adjust the cable, and easy detachment of the muscle from the forearm. Fig. 4, (b) shows the connector and its 3D printed casing for the attachment to three CT-SDEAs' end-plates. The CT-SDEAs, in the artificial skeletal muscle were connected in parallel to a power terminal and were driven by a high voltage (HV) amplifier using a custom LabVIEW program. The active range of motion (ROM), in the sagittal and transverse planes, and angular velocity, in the sagittal plane, were measured under different levels of tensile load, 1 N (the weight of the phantom model's forearm) to 4 N (g=10 m/s^2). Because we were investigating the capability of the artificial muscle in flexing the elbow, any motion in the transverse plane was considered undesirable. Thus, the angular velocity in the transverse plane was not reported.

C. MoCap

ROM and angular velocity were calculated using kinematic data collected by three-dimensional motion capture (MoCap) (Motion Analysis Corp, Santa Rosa, CA, USA) at 128 Hz. Reflective markers were attached to the tip of the hand, shoulder piece, forearm, upper arm, and center of rotation on the phantom model. Eight high-frame-rate IR cameras tracked the motion of the markers during the test conditions. The data were then analyzed offline in Visual 3D (C-motion Inc, Germantown, MD, USA).

The ROM was measured for two separate data collection sessions. During each session, five actuations were recorded under each load, i.e., a total of 10 trials for each load. The mean and standard deviation (SD) of ROM for each load are reported in the Results section.

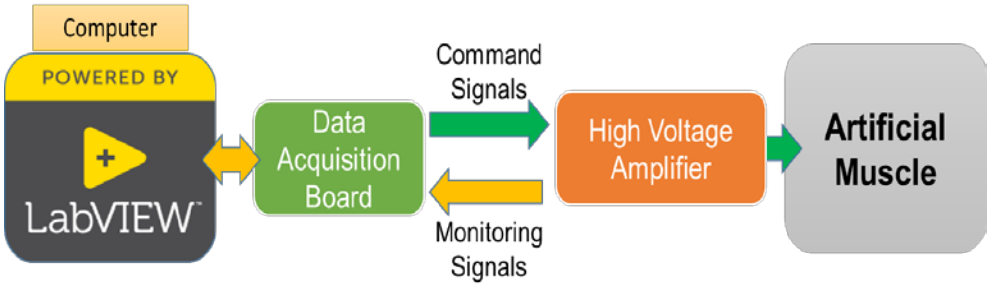

Figure 5. The block diagram of the control and monitoring system for driving the artificial muscles.

D. Control and Monitoring System

The main components of the control and monitoring system were: 1) a HV amplifier (RC250-1.5P, Matsusada Precision Inc., Shiga, Japan) with 1500 V and 165 mA maximum output voltage and current, respectively, to provide the necessary driving voltage, 0-1230 V, for the CT-SDEAs; 2) a CompactDAQ data acquisition system (CDAQ) (CDAQ-9174, National Instrument, Austin, TX, USA), containing an analog output module (NI 9263) and analog input module (NI 9215), for generating the command signal to control the HV amplifier and monitoring its output voltage and current, respectively; 3) software developed in LabVIEW (National Instrument, Austin, TX, USA), to control the CDAQ. Fig. 5 illustrates the block diagram of this system.

III. Results

A. 3x4 Artificial Muscle

When activated by the square voltage waveform, the maximum isometric force generated by the 3x4 artificial muscle was 30.47 N. The shortenings of the 3x4 artificial muscle were 5.3 mm, 5.2 mm, and 5.1 mm for the 0.4 N, 3.3 N, and 6.8 N loads, respectively. A linear additive behavior was roughly observed by adding the CT-SDEs in series. A single CT-SDEA showed 1.3 mm of shortening (Table I), while four CT-SDEAs in series, in the 3x4 artificial muscle, showed 5.3 mm of shortening. Thus, to increase the amount of shortening of the artificial muscle, we added one more actuator to each fiber, myofibril, and tested the 3x5 artificial muscle on the phantom model to potentially increase the maximum ROM. The resultant muscle showed 6.5 mm of shortening.

B. Testing the Artificial Skeletal Muscle Powered Elbow Joint

The active ROM of the elbow joint, powered by the 3x5 artificial muscle, was measured at 19.5º (1.2), mean and (SD), in the sagittal plane, under 1 N of tensile load; as the tensile load increased to 4 N the active ROM decrease to 9.6º (0.8), (Fig. 6). The peak angular velocity of the elbow flexion was measured at 16.2 º/s under 1 N of tensile load. Fig. 7 shows 8.4° (1.7) to 4.6° (0.7) degrees of external rotation of the elbow, in the transverse plane, created while the artificial skeletal muscle was flexing the elbow.

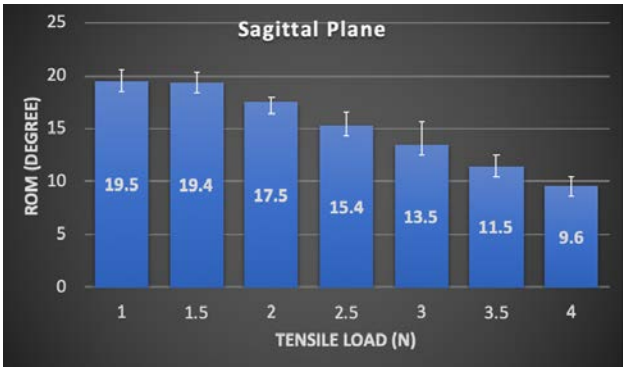

Figure 6. The active range of motion (ROM) of the phantom model's elbow joint, under different levels of tensile loads, in the sagittal plane. The elbow joint is powered by the 3x5 artificial muscle.

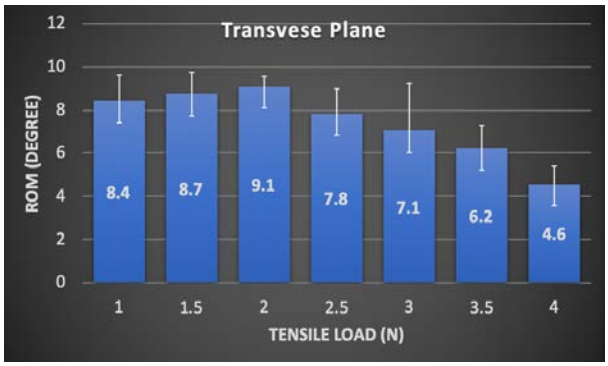

Figure 7. The active range of motion (ROM) of the phantom model's elbow joint, under different levels of tensile loads, in the transverse plane. The elbow joint is powered by the 3x5 artificial muscle.

IV. Discussion

A 3x5 artificial muscle was used to power the elbow joint of a pediatric phantom model. The artificial muscle created 19.5° of elbow flexion, under 1 N tensile load, the load of the phantom model's forearm, with an angular velocity of 16.2°/s. Fast and controlled motion is desirable for exoskeleton applications, however, the reduction in elbow flexion range of motion, at the presence of higher tensile loads may be a substantial hurdle.

Due to the muscle's softness, undesirable deformities were observed during actuation. The generated external rotations (Fig. 7) showed the effect of these deformities and the undesirable motions. This may substantially affect the elbow joint's active ROM, considering the limited contraction of these artificial skeletal muscles, < 6.5 mm. One solution is to confine these artificial skeletal muscles in a low friction and flexible shell, similar to muscle fascia, and attach these muscles to a harder skeletal-like structure to confine these soft actuators' motion in certain directions. In exoskeleton applications, this can be done by highly flexible materials such as silicone films.

Adding a suitable cable-driven mechanical transmission may improve the powered elbow joint's dynamics. Furthermore, the development of an appropriate cable attachment mechanism to magnify displacement of the forearm will be critical for exoskeleton applications. For example, the reported shortening of the biceps muscle in adults is 4 cm [31], where active ROM of the elbow is about 160º, whereas, the artificial muscle tested in this study had 0.65 cm displacement and created only 19.5º of elbow flexion.

As the tensile load increased at the COM of the forearm+hand, from 1 N to 4 N, the degree of elbow flexion was reduced substantially from 19.5° to 9.6°. This is partially due to the extension of the artificial muscle under higher loads because of its softness. This may improve by increasing the lever arm and trading off the ROM at the lighter loads. Due to the flexibility of the actuator, however, bowstringing of the artificial muscle will need to be addressed. Deploying push-pull cables in the design, instead of the wire cable, may also improve the ROM by reducing slack in the cable.

Another limiting factor of the 3×5 artificial muscle is its length, 195 mm, which is longer than the 175 mm upper arm of a 2-year-old. Due to mechanical compliance, however,

these muscles could be bent over the shoulder to help resolve this issue. Further experiments are needed to test this solution. The active ROM of the elbow joint powered by the 3x4 artificial muscle was measured at 18º at a pilot trial. Because 18º is not substantially less than 19.5 º, the 3x4 configuration may be used instead of the 3x5 to resolve the length issue.

V. Conclusion

The capability of CT-DEA-based artificial muscle in actuating an elbow joint of a pediatric exoskeleton was investigated. A 3×5 artificial skeletal muscle was configured and tested on the elbow joint of a phantom model. It was capable of generating 19.5º of elbow flexion. This muscle created 16.2º/s angular velocity about the elbow, which is desirable for exoskeleton applications. The ROM, however, was limited, especially in the presence of a tensile load equal to or more than that of a 2-year-old forearm+hand. Additionally, the 3×5 artificial muscle required an upper arm length of about 195 mm, which is longer than that of a 2-year-old boy. The result of this study suggested that the degree of elbow flexion for an elbow joint actuated by CT-SDEA without a proper transmission system is limited. Therefore, further improvement is necessary to add a suitable transmission system, to adjust the displacement of the muscle at its insertion point.

Acknowledgment

The authors would like to thank Dr. Federico Carpi and Dr. Gabor Kovacs (CTsystems' CEO) for their invaluable technical consultant.

References

[1] R. S. Calabrò *et al.*, "Who May Benefit From Armeo Power Treatment? A Neurophysiological Approach to Predict Neurorehabilitation Outcomes," *PM&R*, vol. 8, no. 10, pp. 971–978, Oct. 2016.

[2] P. Maciejasz, J. Eschweiler, K. Gerlach-Hahn, A. Jansen-Troy, and S. Leonhardt, "A survey on robotic devices for upper limb rehabilitation," *J. Neuroeng. Rehabil.*, vol. 11, no. 1, p. 1, 2014.

[3] D. J. Reinkensmeyer and M. L. Boninger, "Technologies and combination therapies for enhancing movement training for people with a disability," *J. Neuroeng. Rehabil.*, vol. 9, no. 1, p. 1, 2012.

[4] T. Nef, M. Guidali, … V. K.-M.-W. C. on, and undefined 2009, "ARMin-exoskeleton robot for stroke rehabilitation," *Springer*.

[5] P. Lum, … C. B.-J. of, and undefined 2006, "MIME robotic device for upper-limb neurorehabilitation in subacute stroke subjects: A follow-up study," *Dep. Veterans Aff.*

[6] T. Rahman *et al.*, "Design and testing of a functional arm orthosis in patients with neuromuscular diseases," *IEEE Trans. Neural Syst. Rehabil. Eng.*, vol. 15, no. 2, pp. 244–251, 2007.

[7] H. Krebs *et al.*, "Rehabilitation robotics: pilot trial of a spatial extension for MIT-Manus," *J. Neuroeng. Rehabil.*, vol. 1, no. 1, p. 5, Oct. 2004.

[8] S. J. Page, V. Hill, and S. White, "Portable upper extremity robotics is as efficacious as upper extremity rehabilitative therapy: A randomized controlled pilot trial," *Clin. Rehabil.*, 2013.

[9] G. J. Kim, L. Rivera, and J. Stein, "Combined Clinic-Home Approach for Upper Limb Robotic Therapy after Stroke: A Pilot Study," *Arch. Phys. Med. Rehabil.*, 2015.

[10] I. Babik, E. Kokkoni, A. B. Cunha, J. C. Galloway, T. Rahman, and M. A. Lobo, "Feasibility and Effectiveness of a Novel Exoskeleton for an Infant with Arm Movement Impairments," *Pediatr. Phys. Ther.*, vol. 28, no. 3, pp. 338–346, 2016.

[11] J. Stein, K. Narendran, J. McBean, … K. K.-A. journal of, and undefined 2007, "Electromyography-controlled exoskeletal upper-limb–powered orthosis for exercise training after stroke," *journals.lww.com*.

[12] Z. Qian and Z. Bi, "Recent development of rehabilitation robots," *Adv. Mech. Eng.*, vol. 7, no. 2, p. 563062, 2015.

[13] K. A. Shorter, G. F. Kogler, E. Loth, W. K. Durfee, and E. T. Hsiao-Wecksler, "A portable powered ankle-foot orthosis for rehabilitation.," *J. Rehabil. Res. Dev.*, vol. 48, no. 4, 2011.

[14] Y. Matsumoto, Y. Nishida, Y. Motomura, and Y. Okawa, "A concept of needs-oriented design and evaluation of assistive robots based on ICF," in *Rehabilitation Robotics (ICORR), 2011 IEEE International Conference on*, 2011, pp. 1–6.

[15] T. Mirfakhrai, J. D. W. Madden, and R. H. Baughman, "Polymer artificial muscles," *Mater. today*, vol. 10, no. 4, pp. 30–38, 2007.

[16] Q. Pei *et al.*, electroelastomer rolls and their application for biomimetic walking robots," in *Synthetic Metals*, 2003, pp. 246–253.

[17] H. M. Herr and R. D. Kornbluh, "New horizons for orthotic and prosthetic technology: artificial muscle for ambulation," in *Smart structures and materials*, 2004, pp. 1–9.

[18] Y. Bar-Cohen, "Electroactive polymer (EAP) actuators as artificial muscles reality, potential, and challenges," 2004. [Online]. Available: http://public.eblib.com/choice/publicfullrecord.aspx?p=728484.

[19] F. Carpi, D. De Rossi, R. Kornbluh, R. E. Pelrine, and P. Sommer-Larsen, *Dielectric elastomers as electromechanical transducers: Fundamentals, materials, devices, models and applications of an emerging electroactive polymer technology*. Elsevier, 2011.

[20] R. D. Kornbluh, H. Prahlad, R. Pelrine, S. Stanford, M. A. Rosenthal, and P. A. von Guggenberg, "Rubber to rigid, clamped to undamped: toward composite materials with wide-range controllable stiffness and damping," in *Smart structures and materials*, 2004, pp. 372–386.

[21] S. Chiba, "Dielectric Elastomers," in *Soft Actuators*, Springer, 2014, pp. 183–195.

[22] T. A. Gisby, B. M. O'Brien, and I. A. Anderson, "Self sensing feedback for dielectric elastomer actuators," *Appl. Phys. Lett.*, vol. 102, no. 19, p. 193703, May 2013.

[23] F. Carpi, G. Frediani, C. Gerboni, J. Gemignani, and D. De Rossi, "Enabling variable-stiffness hand rehabilitation orthoses with dielectric elastomer transducers," *Med. Eng. Phys.*, vol. 36, no. 2, pp. 205–211, Feb. 2014.

[24] A. Tognetti *et al.*, "Wearable sensory-motor orthoses for tele-rehabilitation," in *Engineering in Medicine and Biology Society, 2003. Proceedings of the 25th Annual International Conference of the IEEE*, 2003, vol. 4, pp. 3724–3727.

[25] F. Carpi, A. Mannini, and D. De Rossi, "Elastomeric contractile actuators for hand rehabilitation splints," in *The 15th International Symposium on: Smart Structures and Materials & Nondestructive Evaluation and Health Monitoring*, 2008, pp. 692705–692710.

[26] I. S. Yoo, S. Reitelshöfer, M. Landgraf, and J. Franke, "Artificial Muscles, Made of Dielectric Elastomer Actuators-A Promising Solution for Inherently Compliant Future Robots," in *Soft Robotics*, Springer, 2015, pp. 33–41.

[27] G. Kovacs, L. Düring, S. Michel, and G. Terrasi, "Stacked dielectric elastomer actuator for tensile force transmission," *Sensors Actuators A Phys.*, vol. 155, no. 2, pp. 299–307, 2009.

[28] A. Behboodi and S. C. K. S. C. K. Lee, "Benchmarking of a Commercially Available Stacked Dielectric Elastomer As an Alternative Actuator for Rehabilitation Robotic Exoskeletons," in *IEEE 16th International Conference on Rehabilitation Robotics (ICORR)*, 2019, pp. 499–505.

[29] D. A. Winter, *Biomechanics and motor control of human movement*. John Wiley & Sons, 2009.

[30] M. de Onis and A. W. Onyango, "WHO child growth standards," *Lancet (London, England)*, vol. 371, no. 9608, pp. 202–204, Jan. 2008.

[31] G. P. Pappas, D. S. Asakawa, S. L. Delp, F. E. Zajac, and J. E. Drace, "Nonuniform shortening in the biceps brachii during elbow flexion," *J. Appl. Physiol.*, 2002.